

BL20B2

Medical and Imaging I

1. Introduction

BL20B2 is a medium-length beamline with a bending magnet source. It is composed of an optics hutch (OH), upstream experimental hutch 1 (EH1) located 42 m from the source, and downstream experimental hutches 2 (EH2) and 3 (EH3) located more than 200 m from the source. EH1 is located in a storage ring building, whereas EH2 and EH3 are located in the Medium-Length Beamline Facility.

BL20B2 is mainly used for X-ray imaging techniques such as X-ray micro-tomography and real-time radiography. In EH1, high-spatial-resolution and fast imaging experiments, which require a high photon flux density, are performed. In comparison, X-ray imaging experiments with a wide field of view are performed in EH2 and EH3 using an X-ray beam with a large cross section. In addition, phase contrast imaging based on a high spatial coherence of the beam generated over a large propagation distance from the source is also performed.

Recently, double-multilayer monochromators (DMMs) for X-ray energies of 40 keV and 110 keV have been installed as a new beamline optical system. DMMs and the existing double-crystal monochromator (DCM) are currently available as monochromator systems in this beamline, and conventional experiments using the DCM can also be performed. As the activities in FY2021, the performance of the DMMs towards ultrafast X-ray imaging and high-resolution X-ray micro-imaging at 110 keV was evaluated.

2. Specifications of DMMs

The DMMs are designed to generate the output X-ray energies of 40 keV and 110 keV. The DMM for 40 keV is primarily intended to capture the high-speed phenomena in the destruction process of the material and improve the image quality in X-ray angiography. In comparison, the DMM for 110 keV is intended to improve the spatial resolution and reduce the measurement time in high-energy X-ray micro-tomography for electrical devices and large fossils. As shown in the FY2020 annual report ^[1], the DMMs are installed in front of and behind the DCM, and 40 keV and 110 keV beams pass through the same height as the monochromatic beam from the DCM. Therefore, the DMMs and the DCM can be switched while the sample and the experimental setup remain at the same position. The DMMs are made of W/B₄C coated on a Si substrate that is 820 mm long, 80 mm wide, and 60 mm thick and has an effective area with a length of 800 mm and a width of 60 mm, and the primary designed parameters are as follows: multilayer period, 3.85 nm (40 keV) and 1.908 nm (110 keV); number of periods, 50 (40 keV) and 200 (110 keV); Bragg angle, 4.29 mrad (40 keV) and 3 mrad (110 keV) ^[2]. Water-cooled metal filters are also installed upstream of the DMMs to remove low-energy components from the total reflection and reduce the heat load on the DMMs. The measured photon flux densities at EH1 were 1.3×10^{12} photons/sec/mm² (40 keV) and 3.9×10^{10} photons/sec/mm² (110 keV). These flux densities are 600 – 800 times higher than that of the monochromatic beam from the DCM.

3. Introduction of BL-774 system

All of the optical components in OH, including the DCM and newly installed DMMs, are controlled by a new beamline control system, the so-called BL-774. BL-774 can be accessed and controlled from a web browser on a PC connected to the BL-USER-LAN. Since it can also be controlled by XML-RPC, it can be operated using a programming language such as Python.

4. Demonstration of ultrafast radiography

As a demonstration of X-ray imaging using the DMMs, ultrafast radiography was conducted at EH1 [3]. To achieve ultrafast imaging, a high-speed camera SA-Z (Photron) was used in the visible-light conversion-type indirect X-ray imaging detector. The X-ray energy was 40 keV, the effective pixel size was 3 μm , and the field of view was 3 mm. A fuse connected to a circuit that can be operated in an overcurrent mode at a specific timing was used to capture its explosion. Figure 1 shows the moment of

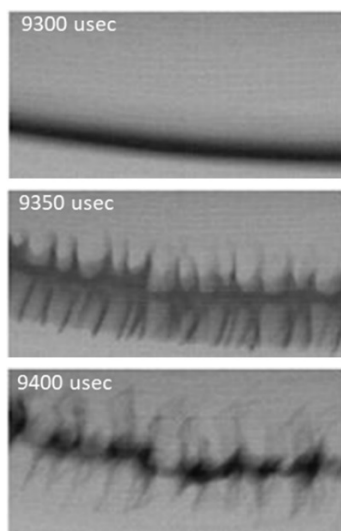


Fig. 1. Fuse explosion observed with 20 kHz. The image width is 3 mm.

fuse explosion. It was confirmed that ultrafast radiography up to 60 kHz can be performed.

5. Demonstration of high-energy X-ray micro-laminography

As a demonstration of high-energy X-ray imaging using the DMMs, high-energy X-ray micro-laminography was conducted at EH2 and EH3. In the previous high-energy experiments using the monochromatic beam from the DCM, poor X-ray photon flux prevented the high-resolution observation [4]. A much-increased photon flux density at 110 keV is expected to achieve high-definition X-ray imaging as well as a reduction in measurement time. In this demonstration, a smartphone was employed as a planar object for high-energy X-ray micro-laminography. Two types of measurement were conducted; one is for the wide-field-of-view observation and the other for the localized high-resolution observation. In the former, the effective pixel size was 12.4 μm and the field of view was 50.8 mm. In the latter, the effective pixel size was 4.2 μm and the field of view was 17.2 mm. A sectional image of the internal circuit board observed in the wide-field-of-view mode is shown in Fig. 2(a). Many structures in the circuit board are clearly observed. A high-resolution image measured at the square region is shown in Fig. 2(b). More detailed structures such as a void in the solder joint are visualized. The measurement time was 35 min even in the high-resolution observation. This is much shorter than in the previous experiment and the image quality is also much improved.

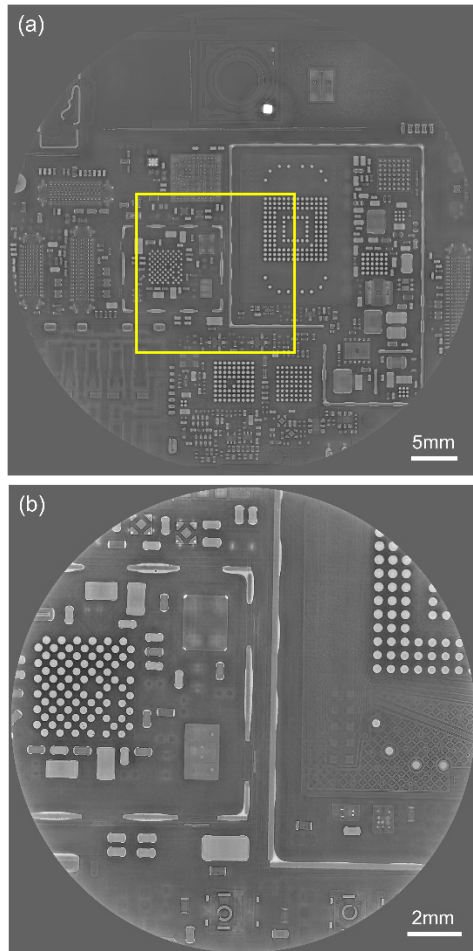


Fig. 2. Sectional images of a circuit board in a smartphone. (a) Wide-field-of-view observation. (b) High-resolution observation at the square region.

6. Conclusion

The DMMs installed as a new optical system are capable of conducting brand new experiments such as ultrafast radiography and high-definition X-ray micro-imaging at 110 keV. In addition to these experiments, high-resolution X-ray micro-tomography with submicron pixel size based on the abundant X-ray photon flux from the DMM for 40 keV will be expected.

Hoshino Masato and Uesugi Kentaro

Japan Synchrotron Radiation Research Institute

References:

- [1] Hoshino, M. & Uesugi, K. (2021). *SPring-8/SACLA Annual Report FY2020*, 52–55.
- [2] Koyama, T. Senba, Y. Yamazaki, H. Takeuchi, T. Tanaka, M. Shimizu, Y. Tsubota, K. Matsuzaki, Y. Kishimoto, H. Miura, T. Shimizu, S. Saito, T. Yumoto, H. Uesugi, K. Hoshino, M. Yamada, J. Osaka, T. Sugahara, M. Nariyama, N. Ishizawa, Y. Nakano, H. Saji, C. Nakajima, K. Motomura, K. Joti, Y. Yabashi, M. & Ohashi, H. (2022). *J. Synchrotron Rad.* **29**, 1265–1272.
- [3] Uesugi, K. Hoshino, M. Koyama, T. Yamazaki, H. Senba, Y. Takeuchi, T. Yumoto, H. Ohashi, H. Yamada, J. Osaka, T. Sugahara, M. & Yabashi, M. (2022). *J. Phys.: Conf. Ser.* Accepted.
- [4] Uesugi, K. & Hoshino, M. (2017). *Proc. SPIE*, **10391**, 103911D.